Control of Collective Network Chaos

Alexandre Wagemakers,[1,*] Ernest Barreto,[2,†] Miguel A. F. Sanjuán,[1,‡] and Paul So[2,§]

[1] *Departamento de Física, Universidad Rey Juan Carlos, Tulipán s/n, 28933 Móstoles, Madrid, Spain*
[2] *Department of Physics, Astronomy, and Computational Sciences and The Krasnow Institute for Advanced Study, George Mason University, Fairfax, Virginia, USA*

(Dated: April 8, 2014)

Under certain conditions, the collective behavior of a large globally-coupled heterogeneous network of coupled oscillators, as quantified by the macroscopic mean field or order parameter, can exhibit low-dimensional chaotic behavior. Recent advances describe how a small set of "reduced" ordinary differential equations can be derived that captures this mean field behavior. Here, we show that chaos control algorithms designed using the reduced equations can be successfully applied to imperfect realizations of the full network. To systematically study the effectiveness of this technique, we measure the quality of control as we relax conditions that are required for the strict accuracy of the reduced equations, and hence, the controller. Although the effects are network-dependent, we show that the method is effective for surprisingly small networks, for modest departures from global coupling, and even with mild inaccuracy in the estimate of network heterogeneity.

The study of the collective dynamics of large populations of coupled oscillators is a vibrant area of research. In 2008 and 2009, Ott and Antonsen published seminal results [1] that made it possible to analytically study the asymptotic behavior of a certain class of such systems. In particular, they showed that under certain conditions, it is possible to derive a set of "reduced" low-dimensional ordinary differential equations that describe the asymptotic behavior of the mean field of such a network. The accuracy of this reduction requires, among other things, that the network of interest consist of infinitely-many oscillators, be globally coupled, and be heterogeneous. The latter condition means that a parameter of the individual oscillators is distributed according to a particular distribution, whose functional form enters into the analysis. These tools have been applied to many systems, including the bimodal [2] and forced Kuramoto systems [3], chimeras [3], etc. Refs. [4] and [5] noted that this analysis permits the study of non-autonomous versions of these networks, as when a network parameter is made to vary sinusoidally in time, and demonstrated that under these circumstances the mean field parameter of the network can exhibit complex behavior including chaos. Here, we apply chaos control techniques [6, 7] to stabilize various unstable periodic orbits that are embedded in a chaotic attractor of the mean field of a non-autonomous network. Control is effected by applying small perturbations to a network parameter. We design the control algorithm based on the reduced equations, but apply the perturbations to a finite realization of the full network. We further investigate the effectiveness of this control method under circumstances in which the accuracy of the reduced equations is compromised in various ways.

I. INTRODUCTION

The study of populations of coupled oscillators has attracted an enormous amount of attention. Nevertheless, it remains a field rich in new discoveries and new applications. Even seemingly elementary systems, such as globally-coupled networks of simple phase oscillators (e.g., the Kuramoto model [8]), are surprisingly powerful models for studying collective network phenomena observed in nature, especially synchronization. Recently, a series of works [1] has shed new light, as it was found that in a wide class of such networks, when the number of oscillators approaches infinity, the macroscopic mean field (or order parameter) converges to a low-dimensional manifold. Furthermore, a small set of ordinary differential equations can be derived that captures the asymptotic behavior of the mean field on this manifold. This astonishing result opens new perspectives into novel applications and analyses of these systems, and several works have resulted [2, 3, 9–11].

For example, in Ref. [4], an extension of the Kuramoto system was studied in which (1) the natural frequency distribution was bimodal, and (2) the overall coupling strength was made to vary sinusoidally in time. For this case, the reduced equation set that describes the asymptotic mean field behavior consists of two non-autonomous ODEs. These equations were used to identify regions of the parameter space for which the network exhibits macroscopic chaos. The same behavior can also be found in a more general class of phase oscillator networks in which the equations of motion can be expressed in "sinusoidally coupled form" [10]. For example, in Ref. [5], chaos and other complex behaviors were also shown to occur in a non-autonomous network of theta neurons.

* alexandre.wagemakers@urjc.es
† ebarreto@gmu.edu
‡ miguel.sanjuan@urjc.es
§ paso@gmu.edu

In this paper, we study three networks drawn from applications that range from the physical to the biological: the two networks described above, i.e., the bimodal Kuramoto network and the theta neuron network [12], as well as a network of coupled Josephson junctions [13]. For the latter system, we establish the occurrence of macroscopic chaotic behavior, in the sense that the mean field or order parameter of the network exhibits chaos.

Our main interest is to apply chaos control techniques to all three systems in order to stabilize various macroscopic unstable periodic orbits. The interest in controlling the network arises in practical situations where the chaotic behavior of the system is undesirable or suboptimal. Alternatively, chaos control offers the possibility of rapidly switching between several of the periodic orbits that are embedded in the uncontrolled chaotic attractor [14]. Some commonly-used network control techniques include pinning [15] and global feedback [16]. In the first method, a small group of nodes is chosen to be controlled, modified or even removed in order to affect the dynamics of the whole network. With the feedback methods, the activity of the whole network is monitored and processed into a control signal that is fed to the network. A recent work [17] showed that an unstable chimera state from a network of identical phase oscillators can be stabilized using a proportional feedback control scheme. Here, we adopt the global feedback approach and describe a method to control the macroscopic chaotic behavior of the network via small changes to one or more accessible network parameters.

The novelty of our approach is that our control strategy is designed using the mean field description of the reduced equation set before it is applied to the actual population of oscillators. This approach has several advantages. A major benefit of this technique is that the control perturbations are calculated using just a few equations, thus avoiding the need to integrate a very large network of coupled differential equations. The latter would be costly or impossible due to the large system size and long simulation time. Furthermore, the controller only requires the state of the macroscopic mean field and at least one accessible network parameter. Thus, if it is possible to measure the mean field of the network directly, then one avoids having to monitor all of the oscillators individually.

A natural question that arises is whether this approach applies to situations in which the accuracy of the reduction described above is compromised. Thus, we check for robustness by examining the effect of finite network size, imperfect global coupling, and inaccuracy in estimating the natural frequency distribution of the network.

II. CONTROL OF COLLECTIVE NETWORK CHAOS: THEORY

A. Macroscopic Reduction of a Sinusoidally Coupled Network

We consider globally-coupled networks of oscillators that can be written in *sinusoidally coupled* form [10], i.e.,

$$\dot{\theta_j} = f(z,t;\Gamma,\eta_j)e^{i\theta_j} + h(z,t;\Gamma,\eta_j) + f^*(z,t;\Gamma,\eta_j)e^{-i\theta_j}. \tag{1}$$

Here, θ_j denotes the phase of the j-th oscillator, $j = 1,\cdots,N$, and $*$ denotes complex conjugation. The collective behavior of the network is quantified by z, the macroscopic mean field or order parameter (defined below), $\Gamma = \{\gamma_a,\gamma_b,\cdots\}$ is a set of network-level parameters, and η_j is an oscillator-level parameter. We assume that our network is heterogeneous in that the parameters η_j are chosen randomly from a time-independent normalized distribution function $g(\eta)$. The key feature of Eq. 1 is that the individual oscillator phase θ_j appears only via the harmonic functions $e^{i\theta_j}$ and $e^{-i\theta_j}$. Particular cases of this general form include, for example, the classic Kuramoto system and many of its extensions [1, 2, 11, 18, 19], the theta neuron network [5, 20], and networks of Josephson junction arrays [9]. Note that this formalism allows the functions f and h to have explicit dependence on time and/or other auxiliary dynamics. As in most statistical reduction methods, the reduced macroscopic mean field equations will, in general, depend on the distribution function g and other network-level parameters, but not on the individual oscillator-level diversity parameters η_j.

Following the mean-field approach pioneered by Kuramoto in 1975 [8] (and later used by many others [21]), we consider the limit $N \to \infty$ and move to a continuum description by introducing a probability density function $\rho(\theta,\eta,t)$ that describes the distribution of the oscillators. Specifically, the quantity $\rho(\theta,\eta,t)d\theta d\eta$ gives the fraction of oscillators whose phases lie in the range $[\theta,\theta+d\theta]$ and whose microscopic diversity parameters lie in $[\eta,\eta+d\eta]$, at a particular time. Since the total number of oscillators is conserved, ρ satisfies the following continuity equation:

$$\frac{\partial\rho}{\partial t} + \frac{\partial}{\partial\theta}\left(\rho v_\theta\right) = 0, \tag{2}$$

where the phase velocity v_θ is given by the continuum version of Eq. 1,

$$v_\theta = f(z,t;\Gamma,\eta)e^{i\theta} + h(z,t;\Gamma,\eta) + f^*(z,t;\Gamma,\eta)e^{-i\theta}. \tag{3}$$

The macroscopic mean-field variable $z(t)$ is a complex quantity given by

$$z(t) = \int_{-\infty}^{\infty}\int_0^{2\pi} \rho(\theta,\eta,t)e^{i\theta}\, d\theta d\eta. \tag{4}$$

If one imagines the state of each individual oscillator being represented by a phasor on the unit circle, the macroscopic mean field $z(t)$ gives the centroid of these phasors.

Writing $z(t) = r(t)e^{i\phi(t)}$, the magnitude $r(t) \in [0, 1]$ characterizes the instantaneous degree of network coherence, and $\phi(t)$ is the instantaneous mean-field phase. Below, we derive a low-dimensional dynamical system whose asymptotic behavior coincides exactly with that of the discrete network described by Eq. 1, with $N \to \infty$.

Many analytical techniques have been developed for the analysis of these systems (e.g., [1–5, 8, 9, 11, 13, 18–20]). Here, we follow the procedure of Ref. [1] and adopt the ansatz that the solution to the continuity equation, Eq. 2, can be written as a Fourier series,

$$\rho(\theta, \eta, t) = \frac{g(\eta)}{2\pi}\left\{1 + \sum_{q=1}^{\infty}\left[\alpha^*(\eta, t)^q e^{iq\theta} + \alpha(\eta, t)^q e^{-iq\theta}\right]\right\}, \tag{5}$$

in which $\alpha(\eta, t)$ is a yet-to-be-determined complex function. In Eq. 5, the amplitudes in the Fourier expansion are monomials in α. This defines a reduced manifold M (parameterized by the real and imaginary parts of α) within the infinite-dimensional space of all possible probability density functions. In [1], Ott and Antonsen showed that this reduced manifold M is invariant for the macroscopic dynamics if and only if α satisfies the differential equation

$$\dot{\alpha} = i(f\alpha^2 + h\alpha + f^*), \tag{6}$$

and $|\alpha(\eta, t)| < 1$ for all time.

The macroscopic mean field can be expressed in terms of α by substituting Eq. 5 into Eq. 4, resulting in

$$z(t) = \int_{-\infty}^{\infty} \alpha(\eta, t)g(\eta)d\eta. \tag{7}$$

We show in Section III that this integral can be evaluated in closed form for our three example systems, and that Eqs. 6 and 7 result in a low-dimensional system of ordinary differential equations for the dynamics on M. Furthermore, it can be shown that M is attracting if the distribution function $g(\eta)$ has a non-zero width [1]. Consequently, these ODEs describe the asymptotic dynamics of the network's macroscopic mean field $z(t)$.

We will refer to these ODEs generically as the "reduced" equations, and for notational convenience, we write them as $\dot{z} = F(z(t))$. Our goal is to develop a parametric control scheme based on this reduced macroscopic model to control collective chaotic states in the full discrete network.

B. Collective Control of Networks

In the cases we consider in this paper, macroscopic chaos can arise (for suitably chosen parameters) in a heterogeneous network when one of the network parameters $\gamma \in \Gamma$ is varied periodically in time, i.e.,

$$\gamma(t) = \gamma_0 + A\sin(2\pi t/\tau), \tag{8}$$

where A is the amplitude and τ is the period. Notably, we assume that γ is a parameter that affects the network as a whole, and not just a subset of the individual oscillators.

We apply the well-known OGY method of chaos control [6, 7, 22] to the reduced mean field model derived in the previous section in order to design our control strategy. Particular low-order unstable periodic orbits (UPOs) of the macroscopic chaotic attractor are targeted to be stabilized with small but carefully chosen perturbations. Since the network is assumed to be driven by a continuous periodic signal of period τ (Eq. 8), we design our controller based on a stroboscopic map $z_{n+1} = \Phi_\tau(z_n)$ of the reduced equations with the same period. This map is obtained numerically from the integration of the reduced ODEs $\dot{z} = F(z)$ over successive time intervals of period τ.

We will refer to periodic orbits as "period-q orbits", where q is a positive integer. By this we mean an orbit of period q on the stroboscopic map Φ_τ; this corresponds to an orbit of period $q\tau$ of the continuous-time ODEs. Unstable period-q orbits embedded within a chaotic attractor correspond to unstable fixed points of q-fold compositions of this stroboscopic map. These can be extracted by solving the equation $\Phi_\tau^q(\bar{z}_i) - \bar{z}_i = 0$ with a modified Newton algorithm [23, 24]. It is important to note that a period-q orbit does not necessarily exhibit q "loops" in the continuous-time state space.

To control an unstable periodic orbit, we use a method described in Ref. [7], which is a slight modification of the original method in [6] that is more appropriate when the period of the orbit is larger than one. First we define the stroboscopic map in terms of r_n and ϕ_n, where

$$z_n = \begin{pmatrix} r_n \\ \phi_n \end{pmatrix} \tag{9}$$

is the nth stroboscopic sampling of the continuous macroscopic mean field $z(t) = re^{i\phi}$. We denote this map as follows:

$$z_{n+1} = \Phi_\tau\left(z_n; p\right), \tag{10}$$

where $p \in \Gamma$ is an accessible macroscopic control parameter of the network.

If a period-q orbit $\bar{z}_{i+q} = \bar{z}_i$ exists in the reduced system for $p = \bar{p}$, the stroboscopic dynamics is linearized around a small neighborhood of the i-th component of the orbit,

$$z_{n+1} - \bar{z}_{i+1} = C_i\left(z_n - \bar{z}_i\right) + D_i\Delta p_n, \tag{11}$$

where $\Delta p_n = p_n - \bar{p}$. Here, the C_i are 2×2 Jacobian matrices and the D_i are two-dimensional column vectors. These characterize the local dynamics along the q consecutive branches of the chosen period-q orbit, and are defined by

$$\begin{aligned} C_i &= D_z\Phi_\tau(z_n; p)|_{z_n=\bar{z}_i, p=\bar{p}} \\ D_i &= D_p\Phi_\tau(z_n; p)|_{z_n=\bar{z}_i, p=\bar{p}} \end{aligned} \tag{12}$$

with $i = 1, \cdots, q$. The right sides of Eqs. 12 are obtained by integrating the linearization of $F(z(t))$, that is, $\dot{\delta}_z = D_z F(z(t))\delta_z$ and $\dot{\delta}_p = D_p F(z(t))\delta_p$, where $D_z F(z(t))$ and $D_p F(z(t))$ are Jacobian matrices computed along the unstable periodic orbit [22]. The integration proceeds from $t = t_0$ to $t_0 + \tau, t_0 + 2\tau, \ldots$, where we chose t_0 to optimize control as described below.

By requiring that the macroscopic orbit land on the stable manifold of the desired periodic orbit, one can write down an explicit condition for the required perturbation of the control parameter:

$$\Delta p_n = \frac{\{C_i \cdot [z_n - \bar{z}_i(\bar{p})]\} \cdot e_{u,i+1}}{-D_i \cdot e_{u,i+1}}, \tag{13}$$

where the column vector $e_{u,i+1}$ is the contravariant vector corresponding to the unstable direction of the $(i+1)$-th component of the period-q orbit. The trajectory is thus driven at each stroboscopic step toward the desired macroscopic period-q orbit from one point to the next with judiciously chosen small perturbations Δp_n. As in all classic chaos control methods, we are utilizing the intrinsic local dynamics of the unstable periodic orbit. Thus, the required parameter perturbations can, in principle, be arbitrarily small (in the absence of noise).

The key idea in this control scheme is that we obtain the control matrices C_i and D_i, and contravariant vectors $e_{u,i}$, using the reduced dynamical system *exclusively*. Then, by stroboscopically sampling the macroscopic mean field z_n of the full discrete network, the collective dynamics of the discrete network can be controlled by applying the perturbations Δp_n as prescribed by Eq. 13.

A controlled trajectory of the stroboscopic map Φ_τ typically remains close to the intended target, but deviates from it iteration by iteration due to finite-population size effects and the limitations of the linearization used in the control scheme. We quantify the efficiency of control by counting the number of iterations for which the controlled trajectory remains within a Euclidean distance ε of a targeted fixed point, and defining the control rate R as the ratio of this number to the total number of iterations in the simulation. In the case of orbits of period $q > 1$, we count in the numerator only those iterations for which the controlled trajectory remains within ε of each of the q components of the orbit. In our simulations, we use $\varepsilon = 0.15$.

III. THREE NETWORK EXAMPLES

In this section, we describe the three networks of phase oscillators which we use to demonstrate the applicability of our collective control scheme. Our networks include an extension of the classic Kuramoto model, a heterogeneous network of canonical Type-I neurons, and a network of nonidentical overdamped Josephson junctions. These examples were chosen to represent a range of applications from neuroscience to physics. In all cases, we choose parameters such that they all exhibit macroscopic chaos in the uncontrolled state.

A. A Bimodal Kuramoto Network

It has been shown that the collective state of a Kuramoto network with bimodal frequency distribution and time-varying coupling can oscillate chaotically [4]. The individual oscillators of the network are defined by the following differential equation:

$$\dot{\theta}_j = \eta_j + \frac{k(t)}{N} \sum_{i=1}^{N} \sin(\theta_i - \theta_j), \tag{14}$$

where $k(t) \in \Gamma$ is a network-level macroscopic parameter that describes the global coupling strength of the network and is assumed to vary periodically in time according to

$$k(t) = k_0 + A \sin(2\pi t/\tau). \tag{15}$$

The diversity parameter η_j gives the natural frequency of the j-th phase oscillator. These are randomly picked from a bimodal Lorentzian distribution,

$$g(\eta; \eta_0, \Delta) = \frac{\Delta}{2\pi} \left(\frac{1}{(\eta - \eta_0)^2 + \Delta^2} + \frac{1}{(\eta + \eta_0)^2 + \Delta^2} \right). \tag{16}$$

This distribution is the sum of two distinct unimodal distributions with central frequencies at $+\eta_0$ and $-\eta_0$, where the half-width at half-maximum of each peak is Δ. The system can be interpreted as two interacting populations of oscillators, with each oscillator being associated with either one or the other unimodal distribution.

To put this network into sinusoidally coupled form, the two mean field coupling functions f and h of Eq. 1 are given by

$$f = \frac{k(t) z(t)}{2i} \tag{17}$$

and

$$h = \eta. \tag{18}$$

Here, $z(t)$ is again the macroscopic mean field variable defined by Eq. 4.

As we have seen, in the thermodynamic limit of an infinite number of oscillators, the OA ansatz yields a pair of integro-differential equations for the asymptotic mean field given by Eqs. 6 and 7. With the choice of Eq. 16 for g, one can evaluate the integral in Eq. 7 in closed form by analytically continuing $\alpha(\eta, t)$ into the upper half of the complex η-plane and evaluating at the residues at $\eta = \pm\eta_0 + i\Delta$. This gives $z(t) = \frac{z_a(t) + z_b(t)}{2}$, where $z_a(t) = \alpha(+\eta_0 + i\Delta, t)$ and $z_b(t) = \alpha(-\eta_0 + i\Delta, t)$ can quite naturally be interpreted as "sub" order parameters that capture the mean fields of the populations in the two-population interpretation of the system.

Then, by evaluating Eq. 6 at the residues and substituting the above expression for $\alpha(t)$, we obtain the following equations for the macroscopic dynamics of the network:

$$\frac{dz_a}{dt} = -z_a(\Delta + i\eta_0) + \frac{k(t)}{4}\left[z_a + z_b - z_a^2(z_a^* + z_b^*)\right] \quad (19)$$

$$\frac{dz_b}{dt} = -z_b(\Delta + i\eta_0) + \frac{k(t)}{4}\left[z_a + z_b - z_b^2(z_a^* + z_b^*)\right]. \quad (20)$$

This system is four-dimensional, and our control scheme could be applied directly at this point. However, we can exploit symmetries inherent in the system and further reduce to two dimensions. Writing $z_x = r_x e^{i\psi_x}$ where $x = a$ or b, the asymptotic behavior of the macroscopic mean field can be written in terms of $r = r_a = r_b$ and the phase difference $\phi = \psi_b - \psi_a$ between the two populations [2]. This yields

$$\frac{dr}{dt} = -\Delta r + \frac{k(t)}{4} r(1 - r^2)(1 + \cos\phi) \quad (21)$$

$$\frac{d\phi}{dt} = 2\eta_0 - \frac{k(t)}{2}(1 + r^2)\sin\phi. \quad (22)$$

In our subsequent investigations, these equations play the role of F with the order parameter redefined as $z(t) = re^{i\phi}$, and stroboscopic samples of r and ϕ from Eqs. 21-22 enter into Eq. 9 when designing the controller.

The autonomous version of this two-dimensional system has a variety of dynamical features and bifurcations, as described in [2]. For the non-autonomous version, it was shown in [4] that for appropriate values of k_0, A, and τ, the collective state of the network can exhibit many complex behaviors including quasi-periodic oscillations, multistability, and chaos.

In Fig. 1, we compare a chaotic trajectory obtained from the reduced system of Eqs. 21-22 to one obtained from the full discrete network of Eqs. 14-16 with 5000 oscillators and the same parameter set. In both cases, we show the time series of the order parameter $z(t) = re^{i\phi}$ in the complex plane. The reduced equation provides an excellent prediction of the asymptotic behavior of the network even for a finite number of oscillators. The trajectory from the discrete network also shows that the dynamics of the population converges rapidly to the OA manifold described by the reduced system.

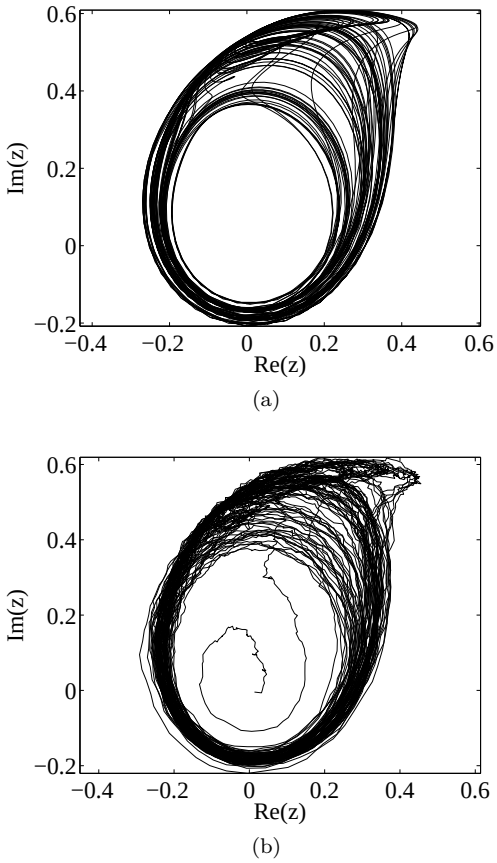

FIG. 1. Chaos in the uncontrolled non-autonomous bimodal Kuramoto network. The trajectories shown are obtained from the reduction (a) and a discrete population (b) of 5000 oscillators. Approximately 100 cycles are shown. Parameters are: $A = 0.65$, $\eta_0 = 1.29$, $k_0 = 4$, $\tau = 5$, $\Delta = 0.8$, and the initial condition used in (b) was near the origin. Notice the noise in (b) due to the finite-size population effect.

B. A Network of Theta Neurons

The theta neuron is the canonical model for neurons with Type-I excitability [12, 25]. Although its properties are different from and are more complex than the simple phase oscillators of the Kuramoto model, the OA reduction method can be applied to networks of theta neurons, yielding another low-dimensional set of ODEs for the asymptotic mean field.

The evolution equation of one theta neuron is

$$\dot{\theta} = (1 - \cos\theta) + (1 + \cos\theta)\,[\eta]\,. \quad (23)$$

This features a saddle-node on an invariant circle (SNIC) bifurcation, where η is the bifurcation parameter. For $\eta < 0$, a stable "resting" equilibrium and an unstable "threshold" equilibrium exist on the invariant circle. At $\eta = 0$ these merge, and for $\eta > 0$, a "spiking" limit cycle exists.

Allowing η to vary slowly in time such that the SNIC bifurcation is traversed periodically results in a model of a parabolically-bursting neuron [12]. We construct a network of such bursters such that each neuron evolves according to

$$\dot{\theta}_j = (1 - \cos\theta_j) + (1 + \cos\theta_j)\,[\eta_j(t) + I_{syn}] \quad (24)$$

where

$$\eta_j(t) = \bar{\eta}_j + A sin\,(2\pi t/\tau + \varphi)\,. \quad (25)$$

Heterogeneity is introduced by randomly drawing $\bar{\eta}_j$ (i.e., the mean value of $\eta_j(t)$) from a distribution $g(\bar{\eta})$. We choose the standard unimodal Lorentzian distribution

$$g(\bar{\eta}) = \frac{1}{2\pi}\frac{\Delta}{(\bar{\eta}-\eta_0)^2+\Delta^2}. \tag{26}$$

The neurons are coupled via I_{syn}, which models pulse-like post-synaptic currents that sum according to

$$I_{syn} = \frac{k}{N}\sum_i^N P_m(\theta_i), \tag{27}$$

where $P_m(\theta) = a_m\,(1-\cos\theta)^m$, $m \in \mathbb{N}$, and a_m is a normalization constant such that

$$\int_0^{2\pi} P_m(\theta)d\theta = 2\pi.$$

The parameter m defines the sharpness of each pulse-like post-synaptic potential, and in this work we restrict consideration to $m = 2$. We assume that the synaptic strength k is the same for all neurons in the network.

The autonomous version of the network defined by Eqs. 24-27 was analyzed in [20], and [5] demonstrated that the non-autonomous version can exhibit macroscopic chaos and other complex behaviors.

In order to write the theta neuron network of Eqs. 24-27 in sinusoidally-coupled form, we first express the rescaled synaptic current (I_{syn}/k) as a function of the mean field z and the synaptic sharpness parameter m as follows:

$$H(z,m) = a_n\left\{B_0 + \sum_{q=1}^{m} B_q\left[z^q + (z^*)^q\right]\right\} \tag{28}$$

with

$$B_q = \sum_{j,l=0}^{m}\delta_{j-2l,q}Q_{jl} \tag{29}$$

and

$$Q_{jl} = \frac{(-1)^{j-2l}m!}{2^j l!(m-j)!(j-l)!}, \tag{30}$$

where $\delta_{i,j}$ is the standard Kronecker delta function on the indices (i,j). Then, the mean field functions f and h of Eq. 1 are given by

$$f = -\frac{1}{2}\left[(1-\eta(t)) - kH(z,m)\right] \tag{31}$$

and

$$h = (1+\eta(t) + kH(z,m)), \tag{32}$$

where $\eta(t)$ is given by Eq. 25.

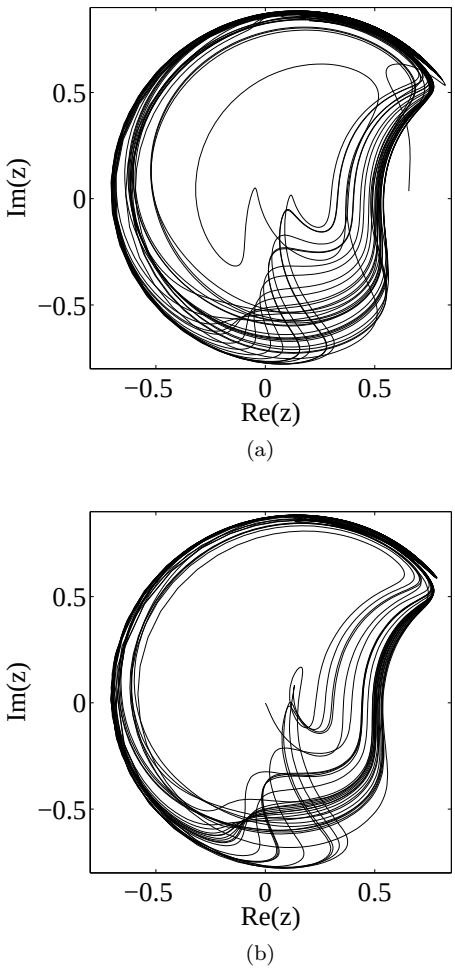

FIG. 2. Chaos in the uncontrolled non-autonomous theta neuron network. The trajectories shown are obtained from the reduction (a) and a discrete population (b) of 5000 oscillators. Approximately 100 cycles are shown. Parameters are: $A = 4.8$, $\eta_0 = 10.75$, $k = -9$, $\tau = 1$, $\Delta = 0.5$.

Finally, by substituting these into Eqs. 6 and 7 and evaluating at the residue $\bar{\eta} = \eta_0 + i\Delta$, we obtain

$$\dot{z} = -i\frac{(z-1)^2}{2} + \frac{(z+1)^2}{2}\left[-\Delta + i\hat{\eta}(t) + ikH(z,m)\right], \tag{33}$$

where

$$\hat{\eta}(t) = \eta_0 + Asin\left(2\pi t/\tau + \varphi\right). \tag{34}$$

This equation plays the role of F in our control scheme, with $z(t) = re^{i\phi}$.

The macroscopic mean field of this theta neuron network exhibits chaos for appropriate parameters, as can be observed in Fig. 2. The prediction from the reduction (Eq. 33), is plotted in panel (a), while the order parameter calculated from a finite population of 5000 theta neurons appears in panel (b).

C. A Network of Josephson Junctions

The circuit equation of a series array of resistively loaded Josephson junctions can be formulated in terms of coupled phase oscillators [9, 13] as

$$\dot{\theta}_j = \beta_j - (1 + b(t)) \cos\theta_j + \frac{1}{N} \sum_{i=1}^{N} \cos\theta_i, \qquad (35)$$

where $b(t) \in \Gamma$ is proportional to the load resistance of the array. Note that the Josephson junction array considered in Refs. [9, 13] was driven by a constant *current*. For our considerations, we prefer to formulate the array such that it is driven by a constant *voltage*, i.e., by an idealized battery. This permits us to allow the load resistance to vary periodically in time while the potential difference across the whole array remains constant. Accordingly, we allow $b(t)$ to vary in time as

$$b(t) = b_0 + A \sin(2\pi t/\tau). \qquad (36)$$

The parameter β_j is inversely proportional to the critical current of the j-th junction, and the set of all critical currents are assumed to be different and distributed according to a unimodal Lorentzian distribution

$$g(\beta) = \frac{1}{2\pi} \frac{\Delta}{(\beta - \beta_0)^2 + \Delta^2}. \qquad (37)$$

To put this into sinusoidal coupling form, the mean field functions f and h of Eq. 1 become

$$f = \frac{1 + b(t)}{2} \qquad (38)$$

and

$$h = \eta + \frac{z + z^*}{2}. \qquad (39)$$

Following the same reduction procedure as described above, the asymptotic macroscopic dynamics for this resistively-loaded overdamped Josephson junction network is given by

$$\frac{dz}{dt} = z(-\Delta + i\beta_0) - \frac{b(t)i}{2}(z^2 + 1) + \frac{i}{2}(|z|^2 - 1), \quad (40)$$

with Eq. 36. Eq. 40 plays the role of F in our control scheme, with $z(t) = re^{i\phi}$.

As with the previous systems, it is possible to find a region of the parameter space where the macroscopic mean field exhibits chaos. In Fig. 3, the numerical integration of the reduction in Eq. 40 is compared with the simulation of the population described by Eq. 35-37. Both simulations are in good agreement with as few as 5000 oscillators in the population.

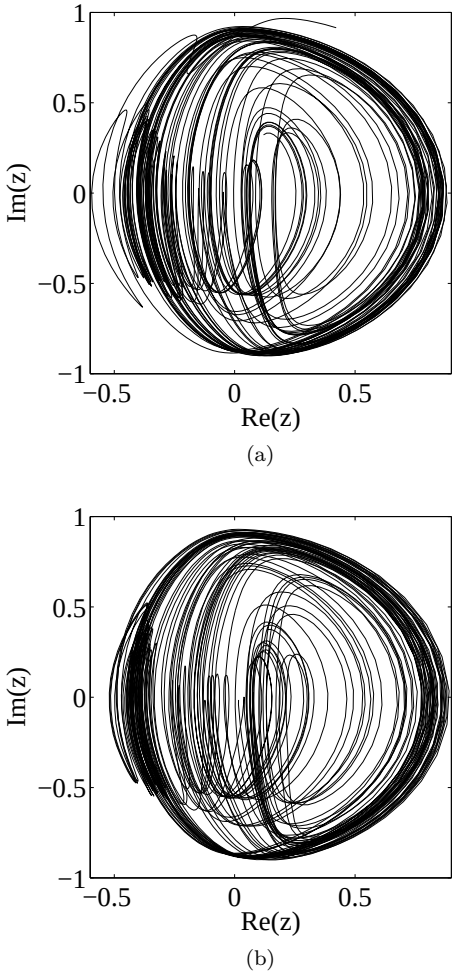

FIG. 3. Chaos in the uncontrolled non-autonomous Josephson junction network. The trajectories shown are obtained from the reduction (a) and a discrete population (b) of 5000 oscillators. Approximately 100 cycles are shown. Parameters are: $A = 1.5$, $\beta_0 = 0.3$, $b_0 = -0.6$, $\tau = 5$, $\Delta = 0.025$.

IV. COLLECTIVE CHAOS CONTROL: RESULTS

The reduced equations for our three example networks, i.e., Eqs. 21-22, 33, and 40, allow us to study the asymptotic behavior of the macroscopic mean field of these networks with ease, without having to directly simulate the full networks themselves. The parameter spaces can be studied numerically and analytically to isolate regions where macroscopic chaos arises, and unstable periodic orbits embedded within a given chaotic attractor can be identified. The design of the controller starts with examining the stability near the desired macroscopic UPO using the reduced mean field equations as described in Sec. II B. Once the matrices C_i, D_i, and the contravariant vector $e_{u,i}$ have been obtained for a given stroboscopic map, control of the full network is effected using

an instantaneous measurement of the mean field of the population and applying control perturbations according to Eq. 13.

A. Control of the Bimodal Kuramoto Network

For the bimodal Kuramoto network example, we used the reduced equations (Eqs. 21-22) to identify four different unstable periodic orbits of periods 1, 2, 3, and 3 embedded in the chaotic attractor shown in Fig. 1. These orbits are shown in the left column of Fig. 4 (i.e., panels a, c, e, and g).

We sought to control these UPOs in a discrete network of 50000 oscillators by applying control perturbations to the average coupling strength k_0; see Eq. 15. The results are shown in the right column of Fig. 4 (i.e., panels b, d, f, and h) for ease of comparison. The controlled orbits are shown in gray. Black dots and arrows indicate the phases at which the controlling perturbations were applied. These instants were chosen by varying t_0 in order to obtain the best possible control. Although both series of figures are in good agreement, we can observe noise in the discrete population trajectories because the population is not infinite in size. Orbits of period larger than 3 were also identified in the reduced system, but their control was not possible in the population, possibly due to these noisy finite-size effects.

B. Control of the Theta Neuron Network

For the theta neuron network, we implemented control using the phase shift φ in Eq. 34, and separately the overall synaptic coupling strength k in Eq. 27. UPOs of period 1, 2, and 3 embedded in the chaotic attractor of Fig. 2 were identified and are shown in the left column of Fig. 5. Controlled trajectories targeting these fixed points using φ and k in a discrete network of 10000 theta neurons are shown in the middle and left columns, respectively. Again, black dots and arrows indicate where controlling perturbations were applied. It is clear that control of these UPOs is not only possible, but is accurate using either of these control parameters. Also, noise due to the finite-size effect is much less apparent in this case.

C. Control of the Josephson Junction Network

For our final example, the Josephson junction network, we chose the mean load resistance of the array, i.e. b_0 in Eq. 36, as the control parameter. UPOs of period 1, 2, and 4 embedded in the chaotic attractor of Fig. 3 were identified and are shown in the left column of Fig. 6. Control of these orbits was successfully realized in a discrete network of 5000 oscillators, and the results are shown in the right column of the same figure. As

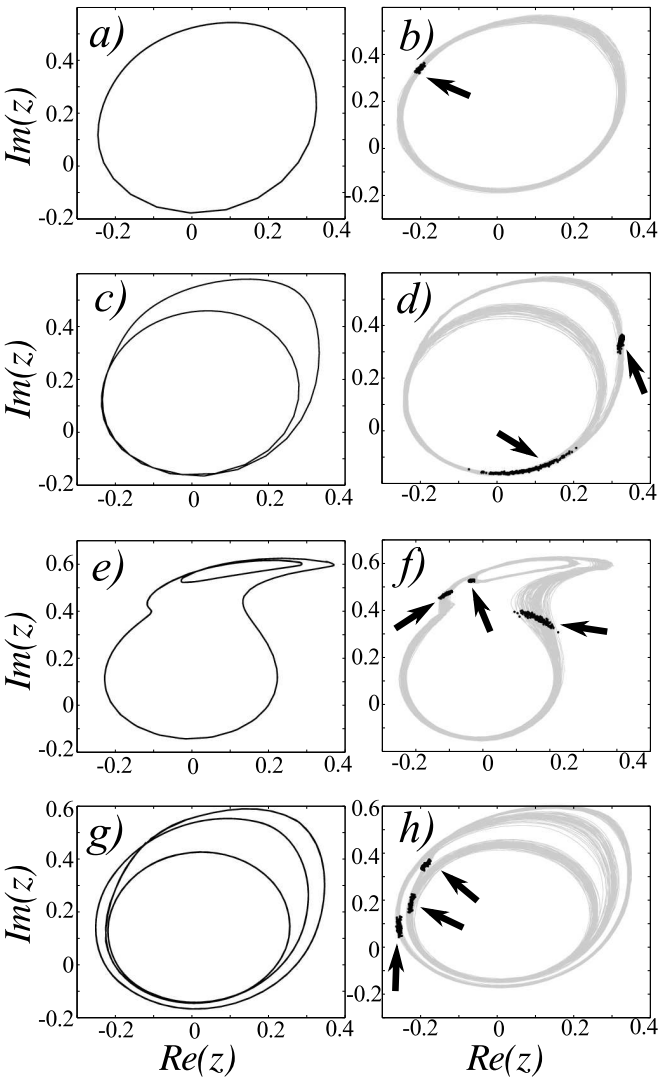

FIG. 4. Control in the chaotic non-autonomous bimodal Kuramoto network. The left column shows four different unstable periodic orbits embedded in the chaotic attractor of Figure 1 that were identified using the reduced equations. These have periods (a) 1, (c) 2, (e) 3, and (g) 3, relative to the stroboscopic map Φ_τ. The right column shows controlled trajectories in a discrete population of 50000 oscillators that target these orbits. Black dots and arrows mark the instants at which controlling perturbations were applied.

in the case of the controlled bimodal Kuramoto system, finite-size effect noise is again apparent. A period 3 orbit was also identified, but we were unable to find a suitable controller for it.

V. NETWORK CHARACTERISTICS AND ROBUSTNESS OF CONTROL

In this section, we address the robustness of our control method. Strictly speaking, the OA reduction method de-

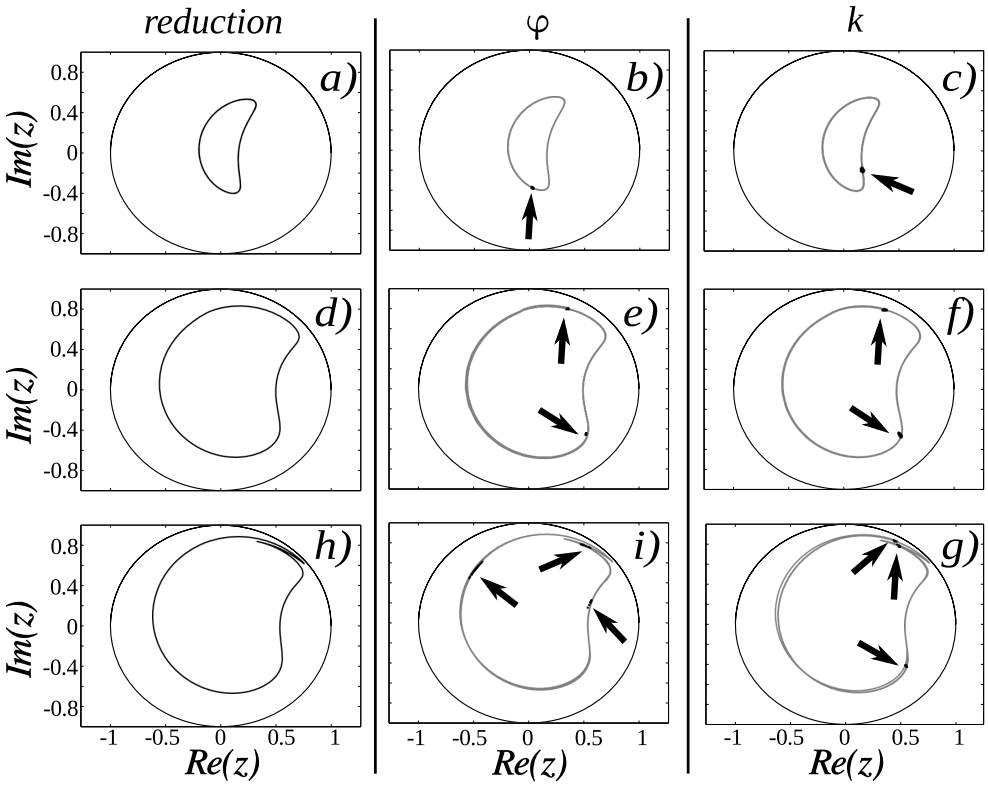

FIG. 5. Control in the chaotic non-autonomous theta neuron network. The left column shows three different unstable periodic orbits embedded in the chaotic attractor of Figure 2 that were identified using the reduced equations. These have periods (a) 1, (d) 2, and (h) 3, relative to the stroboscopic map Φ_τ. The middle and right columns show controlled trajectories in a discrete population of 10000 theta neurons that target these orbits using φ and k as control parameters, respectively. Black dots and arrows mark the instants at which controlling perturbations were applied.

scribed in Section II A, which yields the mean field equations on which our controller is based, requires (1) an infinite number of oscillators, (2) global coupling, and (3) perfect knowledge of the heterogeneity parameter distribution. Here we examine how the control rate R (defined in Section II B) is degraded as each of these assumptions is gradually relaxed.

A. Finite Size Effect

As it evolves in time, the mean field of a network consisting of a finite number of oscillators approximates that of an infinite network, but appears noisy. This is evident in Fig. 1, which compares a chaotic attractor of the infinite non-autonomous bimodal Kuramoto network (obtained via the OA reduction) to the attractor realized by a network of just 5000 oscillators. As the number of oscillators in the finite network is further decreased, this noisy effect becomes more pronounced, and naturally one would expect our control method to fail at some point. Nevertheless, the results presented in Section IV demonstrate that our control method can be successful when applied to non-infinite networks of sufficiently large size.

In Fig. 7 we show how control of the period-1 UPO shown in Figs. 4(a) and (b) degrades as the number of oscillators in the network is decreased from 50000 to 500. We observe that for progressively smaller networks, the controlled orbit deviates more and more from the targeted UPO and instead traces out the chaotic attractor of Fig. 1. In addition, the locations on the trajectory where controlling perturbations are applied (shown by black dots in Fig. 7) become more and more scattered.

We computed the minimum number of oscillators N_{min} necessary to keep a UPO perfectly controlled for all the UPOs that were considered in Section IV above (i.e., those shown in Figs 4-6). We defined perfect control as having a control rate of $R = 1$ for a run of 600 periods. The results are summarized in Table I.

For the bimodal Kuramoto network, only 4000 oscillators are necessary to maintain control of the period-1 orbit at all times, while the period-2 and period-3 UPOs require more than 10000 units to achieve such control. Interestingly, to perfectly control the second period-3 UPO (denoted 3^* in the table), the network must have ten times more oscillators, indicating that this particular orbit is especially vulnerable to the finite-size noise effect.

Both the theta neuron network and the Josephson

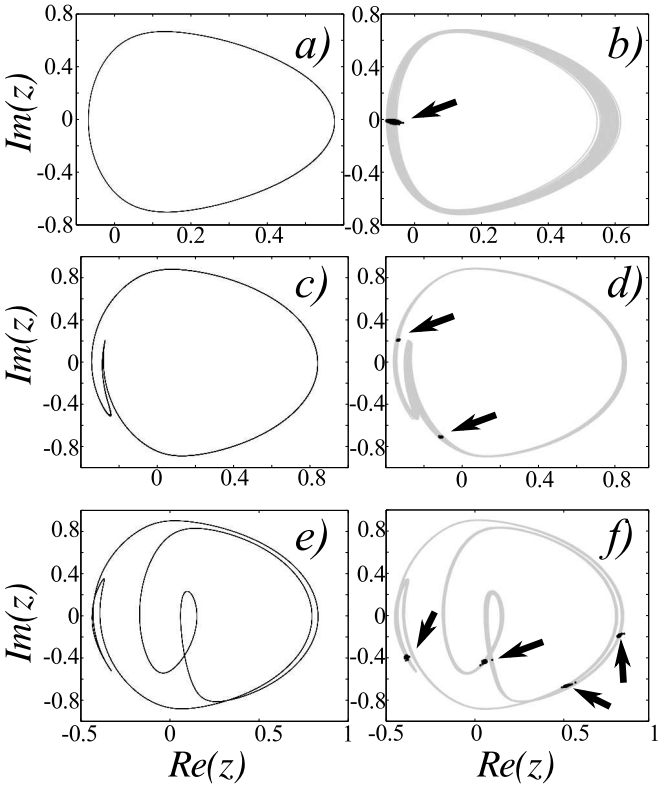

FIG. 6. Control in the chaotic non-autonomous Josephson junction network. The left column shows three different unstable periodic orbits embedded in the chaotic attractor of Figure 2 that were identified using the reduced equations. These have periods (a) 1, (c) 2, and (e) 4, relative to the stroboscopic map Φ_τ. The right column shows controlled trajectories in a discrete population of 5000 oscillators that target these orbits using b_0 as the control parameter. Black dots and arrows mark the instants at which controlling perturbations were applied.

Network	UPO	N_{min}
Bimodal Kuramoto	Period 1	4000
	Period 2	10000
	Period 3	30000
	Period 3*	200000
Theta neuron (φ-control)	Period 1	6000
	Period 2	4000
	Period 3	30000
Theta neuron (k-control)	Period 1	3000
	Period 2	3000
	Period 3	10000
Josephson junction	Period 1	1000
	Period 2	4000
	Period 4	5000

TABLE I. Robustness of control with respect to network size. N_{min} is the number of oscillators in the smallest discrete network for which perfect control of the UPO listed could be achieved. Perfect control was defined as $R = 1$ for 600 cycles.

Network	UPO	Avg. Max. % link removal
Bimodal Kuramoto	Period 1	0.5%
Theta neuron (φ-control)	Period 1	6%
Theta neuron (k-control)	Period 1	2%
Josephson junction	Period 1	4%

TABLE II. Robustness of control with respect to link removal. The right column lists the maximum percentage of link removal for which the average control rate of the listed UPO remains above 0.95.

junction network appear to be less susceptible to the finite-size noise effect than our bimodal Kuramoto network, as is evident by comparing Figs. 1-3. Accordingly, control is more robust with respect to network size in these cases. Interestingly, for the theta neuron network, k-control proved to be more robust to network size than φ-control. Finally, control of the Josephson junction network was the most effective of the examples we studied.

B. Link Removal

Next, we examined the effect of relaxing the requirement that the network be globally coupled by generating networks in which we randomly removed a certain percentage of (bidirectional) links. For brevity, we restricted attention to period-1 orbits. Starting with networks of 10000 oscillators, we constructed five realizations of networks with p-percent link removal, and computed the average control rate $\langle R \rangle_p$ of the period-1 UPO over these networks. We then repeated this procedure, searching for the largest value of p for which $\langle R \rangle_p \geq 0.95$.

Results are shown in Table II. For the bimodal Kuramoto network, effective control of the period-1 orbit is possible with at most 0.5% of the links missing. Compared to the results for the other networks, this is a poor performance; we found that the theta neuron network and the Josephson network were more robust with respect to this manipulation. For the theta neuron network, control fails suddenly around 2% of the total links for the k-controller and around 6% for the φ-controller. It is important to note that for $N = 10000$, 2% link removal corresponds to removing one million out of a total of fifty million links in the globally-coupled network. Finally, results for the Josephson junction network were similar to those of the theta neuron network.

C. Distribution of the Heterogeneous Parameter

Finally, we note that the OA reduction procedure requires perfect knowledge of the heterogeneity parameter distribution in the network of interest, because the functional form of this distribution enters into the derivation of the reduced equations. Recall that the heterogeneity parameters for our example networks are η_j in Eq. 14, $\bar{\eta}_j$

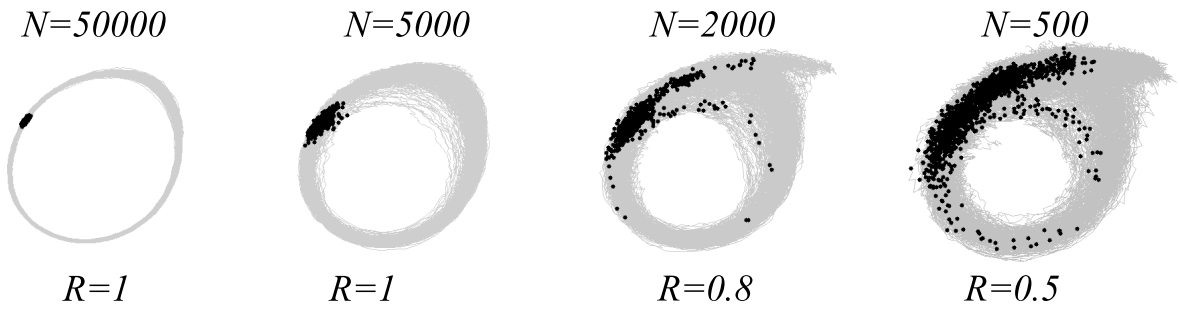

FIG. 7. Example of the degradation of control as the size of the discrete network decreases. The controlled period-1 UPO shown in Figs. 4 (a) and (b) is shown for discrete networks consisting of $N = 50000$, 5000, 2000, and 500 oscillators. Black dots indicate the location at which controlling perturbations are applied. The control rate R for each case is reported below the corresponding figure.

in Eq. 25, and β_j in Eq. 35. In real-world applications, the actual distributions of these or similar parameters may be imperfectly estimated. To test the consequences of this, we prepared two sets of oscillators for each of our example systems in which one set had heterogeneity parameters chosen randomly from a Lorentzian distribution (with parameters η_0 and Δ as in Eq. 26), and the other set had them drawn from a similar Gaussian distribution (with mean η_0 and standard deviation Δ). For our bimodal Kuramoto example system, we used bimodal versions of these distributions, e.g., Eq. 16 and its Gaussian analog. These sets of oscillators were then mixed in varying proportions to form a single network for study. Since the controller is based on the reduced equations, which are derived using Lorentzian distributions, we expected that as the proportion of Gaussian oscillators in the network increased, our control method would eventually fail.

Proceeding as before, we started with networks of 50000 oscillators and constructed five realizations of networks with p-percent Gaussian mixing, and computed the average control rate $\langle R \rangle_p$ of a UPO over these networks. We then repeated this procedure, searching for the largest value of p for which $\langle R \rangle_p \geq 0.95$. Results are shown in Table III.

Network	UPO	max. % of mixing
Bimodal Kuramoto	Period 1	5%
	Period 2	2%
	Period 3	5%
Theta neuron (φ-control)	Period 1	10%
	Period 2	50%
	Period 3	10%
Theta neuron (k-control)	Period 1	80%
	Period 2	60%
	Period 3	50%
Josephson junctions	Period 1	90%
	Period 2	30%
	Period 4	40%

TABLE III. Robustness of control with respect to inaccurate estimation of the heterogeneity distribution. The right column lists the maximum percentage of Gaussian-distributed oscillators in the population for which the average control rate of the listed UPO remains above 0.95.

In the bimodal Kuramoto network, control is effective when the population contains less than roughly 5% of Gaussian-distributed oscillators. Interestingly, we found that when the ratio exceeds 10%, the network behavior abruptly switches to a stable period-1 attractor not related to the originally-targeted orbit. Thus, the mixing procedure leads to a drastic change in the system such that the chaos that one is trying to control no longer exists for sufficiently large mixing. The critical mixing percentage for this kind of failure may depend on the particular implementation of the controller. Nevertheless, our results show that our control algorithm is appreciably robust with respect to ambiguity in the distribution describing the heterogeneous population.

In the theta neuron network, both controllers (k and φ) are able to stabilize the targeted UPOs when the Gaussian-distributed oscillators represent less than 10% of the population. Once again, simulations show that the controlled network switches abruptly to a stable period-1 attractor when the mixing reaches a critical threshold of about 50%, thus indicating the disappearance of the uncontrolled chaotic attractor. We note that the k-controller is more effective against this type of failure as compared to the φ-controller.

Surprisingly, the period-1 UPO in the Josephson junction network was controllable with as much as 90% of the oscillators drawn from the Gaussian distribution. Control of higher-order UPOs was less robust but similar to k-control in the theta neuron network. In both cases, however, control was significantly more robust than in the bimodal Kuramoto case.

VI. CONCLUSION

The collective behavior of a large network of coupled oscillators can be complex or even chaotic. Controlling the microscopic constituents of such a chaotic network can be prohibitively difficult, and it may be more practical to control the macroscopic behavior of the network through a series of small perturbations delivered to an accessible global network parameter. Here, we have shown that efficient control of collective network chaos in this manner is indeed possible.

Recent results have demonstrated that the asymptotic mean field of a certain class of globally-coupled oscillator networks can, in the continuum limit, be fully described by a set of low-dimensional ordinary differential equations. We used this approach to obtain the reduced equations for three example networks, and used them to (1) identify parameter sets for which the networks exhibit chaos, (2) identify several unstable periodic orbits embedded in selected network chaotic attractors, and (3) design a controller based on OGY-type chaos control techniques. Note that doing any of these without the reduced equations would be extremely difficult if not outright impossible.

We then applied this controller directly to realizations of the full discrete network, and demonstrated that targeted UPOs can indeed be stabilized. It was not *a priori* obvious that this approach would be successful. Since the control algorithm is based on the reduced equations, this scheme requires that the reduced dynamical system be a faithful representation of the full discrete network. This is guaranteed only under the assumption of a globally-coupled network consisting of an infinite number of oscillators, with perfect knowledge of the network heterogeneity. But such networks are not possible to either simulate exactly or realize experimentally.

Therefore, we tested the robustness of our control method in networks in which we systematically compromised these three assumptions. Indeed, if the networks had too few oscillators, control would fail. Nevertheless, control was effective and robust in networks of just a few thousand oscillators. Control appears to fail when noise due to the finite population size effect obscures the fine details of the state-space structure of the targeted orbits, such as when different arcs or "loops" of the orbit are very close together. These features occur more commonly in higher-order orbits. Accordingly, we found that control was most effective for low-order UPOs that have a simpler structure.

Similarly, removing too many links from the network led to the failure of control, but again, control was indeed possible for modest departures from global coupling. The same was true for departures from the Lorentzian heterogeneity distribution, which was assumed when designing the controller. It is likely that a noise effect similar to that seen in small networks underlies the initial breakdown of control in these cases. However, we did observe instances of a more catastrophic failure, especially with breakdown of the heterogeneity distribution assumption, in which the overall dynamical structure of the network changed drastically. In these cases, it appears that the chaotic attractor that exists in the ideal network was destroyed and abruptly replaced with an unrelated stable periodic orbit. Thus, departing from the prediction of the reduced equations by gradually relaxing the theory's underlying requirements cannot be expected to be a smooth process.

Finally, we observe that it may be possible to mitigate some of these deleterious effects. For example, we showed that control of our theta neuron network was possible using either the network coupling strength k or the phase shift φ. It is likely that the effectiveness of control can be significantly improved by using both of these parameters together, as was demonstrated in [26].

ACKNOWLEDGMENTS

A.W. acknowledges support from the URJC Scholarship and the hospitality of the Krasnow Institute for Advanced Study at George Mason University. Financial support from the Spanish Ministry of Science and Innovation under Project No. FIS2009-09898 is acknowledged.

[1] E. Ott and T. M. Antonsen, Chaos: An Interdisciplinary Journal of Nonlinear Science **18**, 037113 (2008).
E. Ott and T. M. Antonsen, Chaos: An Interdisciplinary Journal of Nonlinear Science **19**, 023117 (2009).
E. Ott, B. R. Hunt, and T. M. Antonsen, Chaos: An Interdisciplinary Journal of Nonlinear Science **21**, 025112 (2011).

[2] E. A. Martens, E. Barreto, S. H. Strogatz, E. Ott, P. So, and T. M. Antonsen, Phys. Rev. E **79**, 026204 (2009).

[3] L. M. Childs and S. H. Strogatz, Chaos: An Interdisciplinary Journal of Nonlinear Science **18**, 043128 (2008).
D. M. Abrams, R. Mirollo, S. H. Strogatz, and D. A. Wiley, Phys. Rev. Lett. **101**, 084103 (2008).
C. R. Laing, Physica D: Nonlinear Phenomena **238**, 1569 (2009).

[4] P. So and E. Barreto, Chaos: An Interdisciplinary Journal of Nonlinear Science **21**, 033127 (2011).

[5] P. So, T. B. Luke, and E. Barreto, Physica D: Nonlinear Phenomena **267**, 16 (2014).

[6] E. Ott, C. Grebogi, and J. A. Yorke, Phys. Rev. Lett. **64**, 2837 (1990).

[7] C. Grebogi and Y.-C. Lai, in *Handbook of Chaos Control*, edited by H. G. Schuster (Wiley, 2006), p. 120.

[8] Y. Kuramoto, in *International Symposium on Mathemat-*

ical Problems in Theoretical Physics, edited by H. Araki (Springer Berlin Heidelberg, 1975), vol. 39 of *Lecture Notes in Physics*, pp. 420–422, ISBN 978-3-540-07174-7.

[9] S. A. Marvel and S. H. Strogatz, Chaos: An Interdisciplinary Journal of Nonlinear Science **19**, 013132 (2009).

[10] S. A. Marvel, R. E. Mirollo, and S. H. Strogatz, Chaos: An Interdisciplinary Journal of Nonlinear Science **19**, 043104 (2009).

[11] L. M. Alonso, J. A. Alliende, and G. B. Mindlin, The European Physical Journal D **60**, 361 (2010).
W. S. Lee, E. Ott, and T. M. Antonsen, Phys. Rev. Lett. **103**, 044101 (2009).
L. F. Lafuerza, P. Colet, and R. Toral, Phys. Rev. Lett. **105**, 084101 (2010).
T. M. Antonsen, R. T. Faghih, M. Girvan, E. Ott, and J. Platig, Chaos: An Interdisciplinary Journal of Nonlinear Science **18**, 037112 (2008).
C. R. Laing, Chaos: An Interdisciplinary Journal of Nonlinear Science **19**, 013113 (2009).
L. M. Alonso and G. B. Mindlin, Chaos: An Interdisciplinary Journal of Nonlinear Science **21**, 023102 (2011).

[12] G. Ermentrout and N. Kopell, SIAM Journal on Applied Mathematics **46**, 233 (1986).

[13] S. Watanabe and S. H. Strogatz, Physica D: Nonlinear Phenomena **74**, 197 (1994).

[14] E. Barreto, E. J. Kostelich, C. Grebogi, E. Ott, and J. A. Yorke, Phys. Rev. E **51**, 4169 (1995).

[15] X. Li, X. Wang, and G. Chen, Circuits and Systems I: Regular Papers, IEEE Transactions on **51**, 2074 (2004).

[16] M. G. Rosenblum and A. S. Pikovsky, Phys. Rev. Lett. **92**, 114102 (2004).

[17] J. Sieber, O. E. Omel'chenko, and M. Wolfrum, Phys. Rev. Lett. **112**, 054102 (2014).

[18] A. Pikovsky and M. Rosenblum, Phys. Rev. Lett. **101**, 264103 (2008).

[19] A. Pikovsky and M. Rosenblum, Physica D: Nonlinear Phenomena **240**, 872 (2011).

[20] T. B. Luke, E. Barreto, and P. So, Neural Computation **25**, 3207 (2013).

[21] Y. Kuramoto, *Chemical Oscillations, Waves and Turbulence* (Springer, 1984).
J. Crawford, Journal of Statistical Physics **74**, 1047 (1994).
S. H. Strogatz, Physica D: Nonlinear Phenomena **143**, 1 (2000).
J. A. Acebrón, L. L. Bonilla, C. J. Pérez Vicente, F. Ritort, and R. Spigler, Rev. Mod. Phys. **77**, 137 (2005).

[22] E. Ott, *Chaos in Dynamical Systems* (Cambridge University Press, 1993).

[23] J. R. Miller and J. A. Yorke, Physica D: Nonlinear Phenomena **135**, 195 (2000).

[24] P. So, E. Ott, S. Schiff, D. Kaplan, T. Sauer, and C. Grebogi, Phys. Rev. Lett. **76**, 4705 (1996).

[25] B. Ermentrout, Neural Computation **8**, 979 (1996).

[26] E. Barreto and C. Grebogi, Phys. Rev. E **52**, 3553 (1995).